Fracture Analyses of Circumferential Surface Cracked Pipes

Y-J Kim[1], **J-S Kim**[1], **Y-J Kim**[1] and **Y-W Park**[2]

[1] SAFE Research Centre, Sungkyunkwan University, Suwon, KOREA
(E-mail) kimy@nppsafe.skku.ac.kr, (Fax) 81-31-290-5276
[2] Korean Institute of Nuclear Safety, Taejon, KOREA

ABSTRACT: *This paper provides the J estimation equations for circumferential cracked pipes with inner, semi-elliptical surface cracks, subject to internal pressure and global bending. The plastic influence functions for fully plastic J solutions are tabulated based on one hundred and nine 3-D FE calculations using the Ramberg-Osgood (R-O) materials, covering a wide range of pipe and crack geometries. The developed GE/EPRI-type fully plastic J estimation equations are then re-formulated using the concept of the reference stress approach for wider applications. The proposed reference stress based J estimation is then validated against detailed 3-D elastic-plastic, showing excellent agreements. An important aspect of the proposed estimation is that it can be used to estimate J not only at the deepest point of the surface crack but also at an arbitrary point along the crack front.*

INTRODUCTION

Estimating ductile fracture mechanics parameters, such as the *J*-integral, for pipes with part circumferential inner surface cracks, subject to internal pressure and bending moment, is important in structural integrity assessment of defective components. In particular, one important issue for such part through surface crack problems is that the maximum value of crack driving force can occur not only at the deepest point of the crack front but also at an arbitrary point including at the surface point. Thus an engineering scheme should provide estimations of the *J*-integral not only at the deepest point for surface defects but also at an arbitrary point along the crack front including at the surface point.

This paper provides engineering *J* estimation methods for pipes with part circumferential inner surface cracks, subject to internal pressure and global bending. Based on extensive 3-D elastic-plastic FE analyses, relevant plastic influence functions for the GE/EPRI-type approach, which in turn are re-formulated in terms of the tensile strain and stress, based on the reference stress approach.

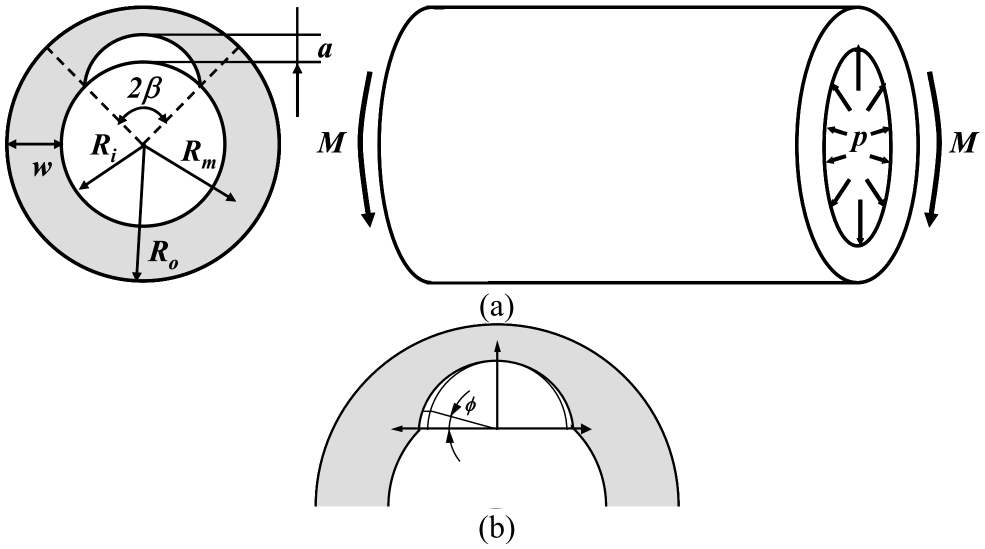

Fig. 1 (a) Schematic illustration of surface cracked pipes under internal pressure p and under global bending M, and (b) definition of the crack angle ϕ.

FE ANALYSIS AND PLASTIC INFLUENCE FUNCTIONS

Detailed 3-D finite element analysis for a part circumferential inner surface crack in a pipe, subject to internal pressure p and global bending moment M, as depicted in Fig. 1, is performed using ABAQUS [1]. To cover practical ranges of these variables, two values of R_m/t were selected, R_m/t=5 and 20; four values of a/t were selected, ranging from a/t=0.1 to 0.75; and three values of β/π were selected, ranging from 0.1 to 0.4. The material in the FE analyses is assumed to follow the Ramberg-Osgood (R-O) relation:

$$\frac{\varepsilon}{\varepsilon_o} = \frac{\sigma}{\sigma_y} + \alpha\left(\frac{\sigma}{\sigma_y}\right)^n \tag{1}$$

where $E\varepsilon_o=\sigma_y$ where E is the Young's modulus, taken as E=200GPa; σ_y denotes the 0.2% proof (yield) stress; and α and n are the R-O parameters. In the present FE analysis, α and σ_y are fixed to α =1 and σ_y=400 (*MPa)*. The values of the strain hardening index, n, however, are systematically varied; n=1 (elastic), 3, 5 and 10. The twenty-node isoparametric quadratic brick elements with reduced integration (C3D20R in ABAQUS) were used to construct a quarter model of the pipe owing to a symmetric condition. The resulting finite element model consists of 1,800 elements with 8,817 nodes, as shown in Fig. 2. The FE modes were subject to two different loading conditions, internal pressure and global bending moment, leading to a total of one hundred and ninety two calculations.

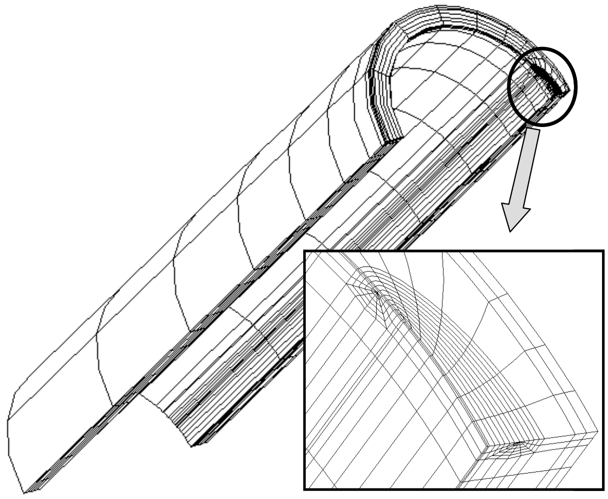

Fig. 2. A typical FE mesh for R_m/t=5, a/t=0.3 and β/π=0.1.

The J-integral values were extracted from the FE results using a domain integral, as a function of the applied internal pressure or the applied global bending moment. For the R-O materials (see Eq. (1)), the fully plastic part of the J-integral, J_p, for pipes with part circumferential inner surface cracks can be expressed as [2]

$$J_p = \alpha \left(\frac{\sigma_y^2}{E} \right) (t-a) \frac{a}{t} h_1(n) \left(\frac{Q}{Q_L} \right)^{n+1} \tag{2}$$

where $h_1(n)$ denotes the plastic influence functions for J_p, Q denotes the generalised load and Q_L is the plastic limit load for Q (either plastic limit pressure, p_L, or the plastic limit moment, M_L) [3]:

$$p_L = \frac{2\sigma_y t}{R_m} \left(1 - \frac{\beta a/t + 2\sin^{-1}[a\sin(\beta)/2t]}{\pi} \right) \tag{3}$$

$$M_L = 4{R_m}^2 t\sigma_y \left(\cos\left[\frac{a\beta}{2t} \right] - \frac{a\sin\beta}{2t} \right) \tag{4}$$

The resulting values of $h_1(n)$ for R_m/t=20 are tabulated in Table 1 for internal pressure and in Table 2 for global bending. More results for $h_1(n)$

can be found in Refs. [4,5].

Table 1. Values of $h_1(n)$ for the *J*-integral, (internal pressure).

R_m/t	a/t	β/π	n			
			1	3	5	10
20	0.1	0.1	4.57	11.88	33.16	478.45
		0.25	4.35	10.59	27.81	346.69
		0.4	4.15	9.60	23.87	261.80
	0.3	0.1	7.92	21.67	57.62	687.70
		0.25	7.05	16.29	36.25	274.53
		0.4	6.07	12.01	22.60	113.87
	0.5	0.1	15.20	41.95	103.55	1011.90
		0.25	13.52	29.14	53.69	239.60
		0.4	10.34	16.99	22.92	47.47
	0.75	0.1	34.85	93.03	224.03	1881.42
		0.25	34.05	60.56	93.75	253.60
		0.4	21.58	23.73	21.24	17.07

Table 2. Values of $h_1(n)$ for the *J*-integral (global bending).

R_m/t	a/t	β/π	n			
			1	3	5	10
20	0.1	0.1	6.44	6.65	6.56	5.95
		0.25	6.25	6.43	5.73	5.37
		0.4	6.14	6.21	5.40	4.65
	0.3	0.1	11.51	16.69	18.34	21.08
		0.25	10.73	14.64	15.12	14.69
		0.4	9.83	12.35	11.60	9.16
	0.5	0.1	22.66	35.12	35.59	35.25
		0.25	21.43	30.36	27.54	20.30
		0.4	17.87	22.21	17.44	9.09
	0.75	0.1	53.42	68.74	73.14	77.53
		0.25	55.85	63.79	58.12	32.76
		0.4	39.03	34.95	23.29	6.12

REFERENCE STRESS FORMULATION

The elastic part of J can be expressed as

$$J_e = \frac{K^2}{E'} = \left(\frac{\sigma_y^2}{E} t\right) h_1(n=1) \left[\frac{Q}{Q_L}\right]^2 \tag{5}$$

where $h_1(n=1)$ denotes the value of $h_1(n)$ for the elastic (n=1) material. Present elastic FE results provide values of elastic J, from which values of

$h_1(n=1)$ can be found, as tabulated in Table 1 for internal pressure and in Table 2 for bending. Normalising Eq. (5) with respect to Eq. (2) gives

$$\frac{J_p}{J_e} = \alpha \frac{h_1(n)}{h_1(n=1)} \left[\frac{Q}{Q_L} \right]^{n-1} \tag{6}$$

Variations of $h_1(n)/h_1(n=1)$, determined from the present FE results, with the strain hardening index n can be easily obtained. Detailed results for $h_1(n)/h_1(n=1)$ can be found in Refs. [4,5], but it would be sufficient to note sensitivity of $h_1(n)/h_1(n=1)$ to n. For internal pressure, the values of $h_1(n)/h_1(n=1)$ range from 1 to ~50 for n ranging from 1 to 10, whereas for bending they range moderately from 0.5 to 2.

Introducing another normalising load Q_{ref} instead of Q_L, and re-phrasing Eq. (6) gives

$$\frac{J_p}{J_e} = \alpha \left\{ \frac{h_1(n)}{h_1(n=1)} \left[\frac{Q_{ref}}{Q_L} \right]^{n-1} \right\} \left[\frac{Q}{Q_{ref}} \right]^{n-1} = \alpha H_1 \left[\frac{Q}{Q_{ref}} \right]^{n-1} \tag{7}$$

where H_1 is generally a function of geometry and n. The underlying idea of the reference stress based approach is that a proper definition of Q_{ref} can minimise the geometry and n dependence of H_1 in Eq. (7) [6]. Suppose that such load has been found. This particular reference load will be referred to as the optimised reference load, Q_{OR} (p_{OR} or M_{OR}), in the present paper. Based on the FE results given in the previous section, the following expressions are proposed for Q_{OR}:

$$p_{oR} = \left[1.767 \left(\frac{a}{t} \right) \left(\frac{\beta}{\pi} \right) - 0.156 \left(\frac{a}{t} \right) - 0.101 \left(\frac{\beta}{\pi} \right) + 0.627 \right] p_L \tag{8}$$

$$M_{oR} = \left[\theta_1 \left(\frac{a}{t} \right)^2 + \theta_2 \left(\frac{a}{t} \right) + 1.04 \right] M_L \tag{9}$$

$$\theta_1 = 4.26 \left(\frac{\beta}{\pi} \right)^2 - 1.35 \left(\frac{\beta}{\pi} \right) + 0.80 \ ; \ \theta_2 = -2.30 \left(\frac{\beta}{\pi} \right)^2 + 1.57 \left(\frac{\beta}{\pi} \right) - 0.77$$

where the expressions for p_L and M_L can be found from Eqs. (3) and (4).

Introducing these expressions for $Q_{ref}=Q_{oR}$ into Eq. (7) gives the values of H_1. It has been found that sensitivities of the $h_1(n)/h_1(n=1)$ to n are significantly reduced in H_1, by the use of the optimised reference load solutions [4,5]. Furthermore, the values of H_1 are found to be now closer to unity for all cases, which leads to the following approximation:

$$\frac{J_p}{J_e} \approx \alpha \left[\frac{Q}{Q_{oR}} \right]^{n-1} \tag{10}$$

Noting that this equation is valid for the R-O materials, Eq. (10) can be written explicitly in terms of the strain and the stress

$$\frac{J_p}{J_e} \cong \frac{E\varepsilon_{ref}}{\sigma_{ref}} \quad ; \sigma_{ref} = \frac{Q}{Q_{oR}} \sigma_y \tag{11}$$

In Eq. (11), σ_{ref} is the reference stress and ε_{ref} is the true strain at $\sigma=\sigma_{ref}$, determined from the true stress-strain data. One notable point is that the use of Eq. (11) is not restricted to the R-O materials and is general for any arbitrary stress-strain relationships.

Equation (11) gives the estimate of the plastic J-integral, J_p, and the total J-integral can be estimated by adding the elastic component with plasticity correction [6,7]:

$$\frac{J}{J_e} = \frac{E\varepsilon_{ref}}{\sigma_{ref}} + \frac{1}{2} \left(\frac{\sigma_{ref}}{\sigma_y} \right)^2 \frac{\sigma_{ref}}{E\varepsilon_{ref}} \quad ; \sigma_{ref} = \frac{Q}{Q_{oR}} \sigma_y \tag{12}$$

where the expression of Q_{oR} (either p_{oR} or M_{oR}) can be found from Eq. (8) and Eq. (9), respectively.

COMPARISONS WITH FE RESULTS

FE Analyses Based on Incremental Plasticity

To validate the proposed J estimates, further FE analysis was performed using incremental plasticity. Regarding material properties, actual experimental stress-strain data for two different materials were considered: SA312 Type 304 at the temperature of T=50°C and SA312 Type 316 stainless steels at T=288°C, extracted from test data for Korean nuclear piping integrity program [8]. For a given material, the experimental true stress-plastic strain data were directly given in the FE analysis. Materials were modelled as isotropic elastic-plastic materials that obey the incremental plasticity theory, and a small geometry change option was invoked.

Results

Fig. 3 compares the FE J results for the Type 304 material under internal pressure and global bending, with the proposed reference stress based J estimate for various values of a/t and β/π. Note that the proposed method will be denoted as the enhanced reference stress method ("ERSM") in the subsequent figures. Excellent agreement between the FE results and the proposed J estimates can be seen for all cases considered. Note that these results are at the deepest point along the crack front ($\phi=\pi/2$).

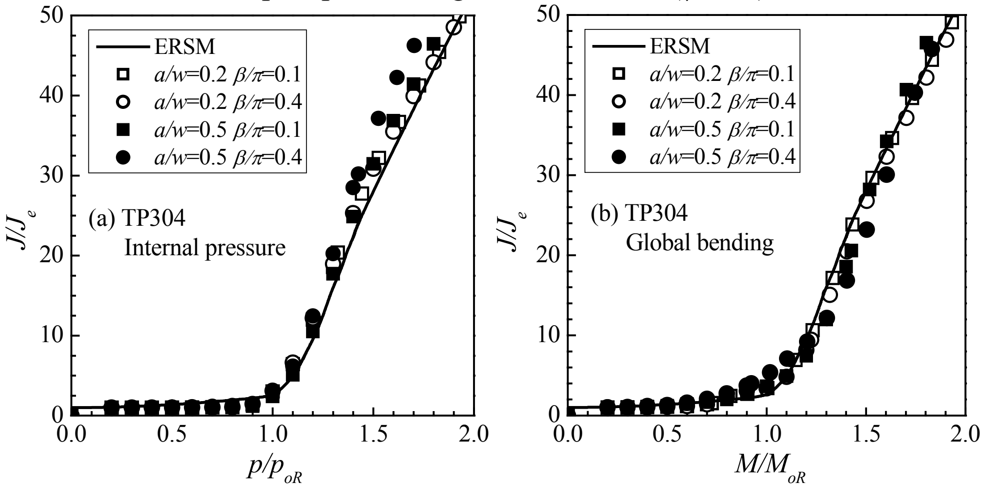

Fig. 3. Comparison of the FE J results with the proposed J estimates for the Type 304 material with R_m/t=20: (a) internal pressure and (b) global bending. Note that the J values are calculated at the deepest point ($\phi=\pi/2$).

To investigate validity of the proposed J estimates to arbitrary points along the crack front, the FE J results at some discrete points along the crack front (including the surface point, ϕ=0) are compared with the proposed J estimates in Fig. 4. Note that in the proposed J estimates, the relevant elastic J along the crack front should be used. The J values in Fig. 4 were normalised with respect to the crack dimension and the yield strength of the material as follows:

$$J_n = \frac{J}{\sigma_y (t-a)(a/t)} \tag{13}$$

Again, agreement between the FE results and the proposed J estimates is excellent not only at arbitrary points along the crack front but also at the surface point.

CONCLUSIONS

This paper provides the reference stress based J estimates for pipes with part circumferential inner surface cracks under internal pressure and under global bending. Comparison with the results from detailed elastic-plastic FE analysis shows excellent agreement. More importantly, it has been shown that, despite its simplicity, the proposed estimation equation can be used to estimate J not only at the deepest point of the surface crack but also at an arbitrary point along the crack front. Such result is significant in practical applications. Excellent agreement shown in this paper provides sufficient confidence in the accuracy of the proposed method, and thus in application to defect assessment of surface cracked pipes.

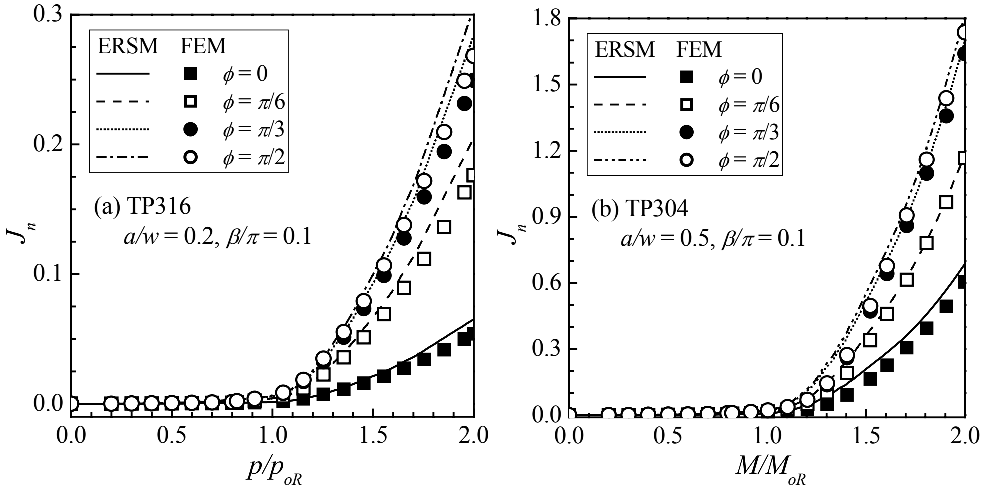

Fig. 4. Comparison of the FE J results at various points along the crack front (ϕ=0, π/6, π/3 and π/2) with the proposed method: (a) pressure, (b) bending.

ACKNOWLEDGEMENT: The authors are grateful for the support provided by a grant from the SAFE Centre at Sungkyunkwan University.

REFERENCES

[1] ABAQUS Version 5.8. User's manual. Hibbitt, Karlson & Sorensen, Inc, RI; 1999.

[2] Kumar V, German MD. EPRI Report, NP-5596, 1988.

[3] Miller A G. Int Jnl of Pressure Vessels and Piping 1988; 32: 191-327.

[4] Y-J Kim et al., Fracture analyses of circumferential surface cracked pipes: part I. International Journal of Fracture (Accepted)

[5] Y-J Kim et al., Fracture analyses of circumferential surface cracked pipes: part II. International Journal of Fracture (Accepted)

[6] Ainsworth RA. Engineering Fracture Mechanics 1984; 19: 633-642.

[7] R6: Assessment of the integrity of structures containing defects, revision 3. British Energy Generation Ltd., 1999.

[8] Kim YJ, Suh MW, Jun HK, Park YW, Choi YH. Nuclear Engineering and Design;174:69-78 (1997).